Canadian Mineralogist
Vol. 16, pp. 37-52 (1978)

THE CRYSTAL CHEMISTRY OF THE AMPHIBOLES. VI. THE STEREOCHEMISTRY OF THE OCTAHEDRAL STRIP

F. C. HAWTHORNE
Department of Earth Sciences, University of Manitoba, Winnipeg, Manitoba R3T 2N2

Abstract

The relationships between mean bond length and mean constituent cation and anion radii are linear for the *M*(1), *M*(2) and *M*(3) octahedra in the clinoamphiboles. Mean bond-length variations are not materially affected by octahedral distortion. Individual bond lengths are controlled by the anion bond-strength requirements, the O(4) anion being of particular importance in this respect. *A priori* bond-length calculations using the method of Baur (1970) result in bond lengths that are systematically larger than the observed values. This correlates with the fact that the observed bond lengths are smaller than those forecast by summation of constituent ionic radii.

In general, shared edges are shorter than unshared edges, in agreement with Pauling's third rule. However, additional geometrical effects also affect bond-angle variations. Packing considerations require that bond angles at *M*(1) and *M*(3) be affected by the *M*(2) cation occupancy; this correlation is observed. Similarly, *M*(2)–O bond-length variations due to local bond-strength requirements strongly affect bond angles in the *M*(2) octahedron.

Sommaire

Les relations entre la longueur moyenne des liaisons et les rayons moyens cationique et anionique sont linéaires pour les octaèdres *M*(1), *M*(2) et *M*(3) dans les clinoamphiboles. La variation de la longueur moyenne des liaisons est à peine affectée par la distortion de l'octaèdre. La longueur des liaisons individuelles dépend fortement des exigences de l'anion quant à la force de la liaison, particulièrement l'anion O(4). Le calcul *a priori* des longueurs de liaisons selon la méthode de Baur (1970) donne des valeurs systématiquement plus grandes que les longueurs observées, résultat lié au fait que la valeur observée est plus courte que la somme des rayons ioniques. En général, les arêtes partagées sont plus courtes que les arêtes non-partagées, ce qui découle de la troisième règle de Pauling. Cependant, d'autres effets géométriques affectent aussi l'angle entre les liaisons. Les règles de l'empilement font que les angles entre liaisons en *M*(1) et *M*(3) dépendent de la population de l'octaèdre *M*(2); cette corrélation est observée. De même, les variations en longueur des liaisons *M*(2)–O, dues aux exigences locales quant à la force de liaison, influencent fortement les angles entre liaisons dans l'octaèdre *M*(2).

(Traduit par la Rédaction)

Introduction

The amphibole structure is formed of two basic elements, the octahedral strip and the tetrahedral chain, both of which extend infinitely along the *c* axis. These two elements link together in the *b* direction by sharing polyhedron corners to form a staggered sheet parallel to the *b-c* plane. These sheets stack together along the *a* axis, being linked by corner-sharing between the individual tetrahedral and octahedral strips. The *M*(4) site occurs at the junction of the two elements and sandwiched between the 'back-to-back' double chains is the *A* site, a large cavity surrounded by twelve anions. The resulting arrangement may be conveniently considered as a sheet structure composed of alternating octahedral and tetrahedral layers (Thompson 1970; Papike & Ross 1970), where space-group variation is a function of the stacking sequence along the *a* axis.

There have been many investigations into the stereochemical variations in the double-chain element of the amphibole structure (Gibbs 1969; Brown & Gibbs 1969, 1970; Mitchell *et al.* 1970, 1971; Baur 1970, 1971). However, apart from studies concerning the ordering of cations in amphiboles (Ghose 1965; Whittaker 1971), the octahedral strip has received little attention. In this study, the stereochemistry of the octahedral strip is examined and an attempt is made to relate these variations to current theories in crystal chemistry. Table 1 lists the structures from which the data were taken for this study. The basic clinoamphibole structure in Figure 1 may be used to identify the various structural parameters discussed, and a glossary of the symbols used here is presented in appendix form. Ionic radii are taken from Shannon & Prewitt (1969, 1970).

Variation in Mean Bond Lengths

In many groups of isomorphous structures, the variation in the mean bond lengths of cation polyhedra may be related to the mean ionic radius of the cations occupying the sites. Thus the variations in the mean octahedral bond lengths

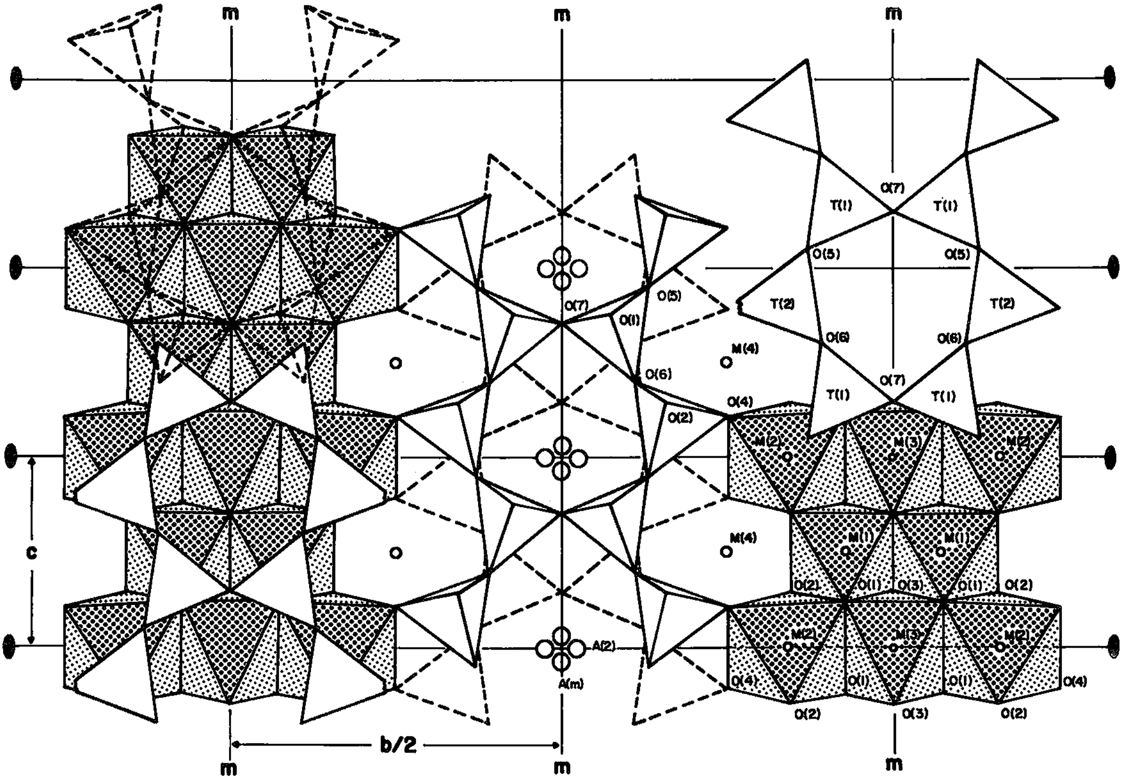

FIG. 1. Polyhedral representation of the clinoamphibole structure, projected down a^*.

in silicate garnets (Novak & Gibbs 1970), olivines (Brown 1970) and alkali pyroxenes (Hawthorne & Grundy 1974, 1977c) are linear functions of the variation in constituent-cation radius. Where this relationship is well-characterized, it is extremely useful in deriving complete site-occupancies when the results of a site-occupancy refinement do not give a unique solution. This situation arises in a crystal-structure refinement either where the two cations present have similar scattering powers or where more than two cations are disordered over two or more sites. Because exact site-occupancies are of interest as potential geothermometers/geobarometers and also are crucial to an understanding of the general crystal chemistry of a mineral group, it is desirable to develop relationships of this sort for application to the more complex chemical variants.

TABLE 1. REFINED CLINO-AMPHIBOLE STRUCTURES USED IN THIS STUDY

Actinolite	Mitchell (1970); Mitchell et al. (1970, 1971)
Al-hastingsite	Hawthorne (1973); Hawthorne & Grundy (1977a)
Cummingtonite	Ghose (1961); Fischer (1966); Mitchell et al. (1971)
Ferrotschermakite	Hawthorne (1973); Hawthorne & Grundy (1973a)
Glaucophane	Papike & Clark (1968); Papike et al. (1969)
Grunerite	Finger (1967, 1969); Finger & Zoltai (1967)
K-richterite	Papike et al. (1969); Cameron (1970)
Kaersutite	Kitamura & Tokonami (1971); Kitamura et al. (1975)
Kakanui hornblende	Papike & Clark (1967); Papike et al. (1969); Robinson (1971); Robinson et al. (1973)
Mn-cummingtonite	Papike et al. (1969)
Na-Fe richterite	Cameron (1970); Cameron & Gibbs (1971)
Na-richterite	Cameron (1970); Cameron & Gibbs (1971)
Oxy-kaersutite	Hawthorne (1973); Hawthorne & Grundy (1973b)
Pargasite	Robinson (1971); Robinson et al. (1969, 1973)
Ti-pargasite	Robinson (1971); Robinson et al. (1973)
Tremolite (F)	Cameron (1970); Cameron & Gibbs (1973)
Tremolite (OH)	Papike et al. (1969)
Tremolite	Hawthorne (1973); Hawthorne & Grundy (1976)
Zincian tirodite	Hawthorne (1973); Hawthorne & Grundy (1973c, 1977b)

Difficulties arise when attempting to derive these relationships for the amphiboles, as accurate site-populations are needed to derive the initial relationships. Few amphiboles have a sufficiently simple chemistry that unique site-populations may be directly derived solely from X-ray structure refinement, and assumptions concerning the site-occupancy of certain cations are necessary in the refinement procedure. The problems involved in complete site-population characterization are:

(i) Accurate chemical analyses are required in order to calculate the cell contents. Errors in analysis (including the presence of contaminating phases) and incomplete analyses (Borg 1967) can lead to incorrect *assigned* site-populations and incorrect bulk chemical constraints in the refinement procedure. Problems of this kind are frequently encountered (Finger 1970; Seifert & Virgo 1975; Whittaker 1969; Irusteta & Whittaker 1975; Papike & Ross 1970; Finger & Ohashi 1974).

(ii) As many as six cation species occur at the octahedral sites in clinoamphiboles; these usually fall into two groups, those with scattering factors similar to Mg (Mg and Al) and those with scattering factors similar to Fe (Fe^{2+},Fe^{3+}, Ti and Mn). Site-occupancy refinement gives only the relative ordering of these two "compound species". Charge-balance criteria (Whittaker 1949; Ghose 1965) and observed mean bond lengths in unoxidized amphiboles indicate that the trivalent cations tend to be ordered into the $M(2)$ octahedron. However, it is not apparent if this ordering is complete (Burns & Greaves 1971; Greaves *et al.* 1971; Hawthorne & Grundy 1977a); it should be noted that post-equilibration oxidation could also lead to Fe^{3+} at the $M(1)$ and $M(3)$ sites. Similar difficulties are encountered with Ti (Ti^{3+} and Ti^{4+}) and the possible effect of pre- and post-equilibration oxidation. The relative ordering of Fe^{2+} and Mn is not well-characterized and has received little attention, although in principle it may be resolved by combined X-ray and Mössbauer investigations (Hawthorne & Grundy 1977b).

(iii) Cations may be partitioned between the $M(4)$ site and the octahedral sites. For the ferromagnesian amphiboles, this may occur for Mn, Fe^{2+} and Mg and site-populations may be derived by combined X-ray and Mössbauer investigations (Hawthorne & Grundy 1977b). For the calcic amphiboles, ΣY type cations commonly exceed 5.0 atoms p.f.u., indicating $M(4)$ occupancy by the smaller divalent cations, and thus occupancy refinement requires consideration of all four M sites. For the sodic amphiboles, examination of a large number of analyses suggests that Na might occur as a Y type cation in small amounts (Hawthorne 1976); however, these arguments could be influenced by the paucity of chemical analyses that include Li_2O, as both chemical (Lyons 1976) and X-ray evidence (Hawthorne, in prep.) indicate that Li occurs at the octahedral sites in the sodic clinoamphiboles.

The factors outlined above emphasize that the following discussion is necessarily somewhat subjective, and that the conclusions can only be regarded as tentative, to be modified when data on more precisely characterized amphiboles become available. In order to develop the relationship between mean bond length and mean ionic radius, it is necessary to make certain assumptions concerning the site-occupancies of particular cation species. There is little evidence concerning some of the cation species involved and the site-occupancy assignments are naturally somewhat arbitrary. The following scheme was used: (i) all Ti was assumed to be trivalent, except in oxy-amphiboles, where it was assumed to be quadrivalent; (ii) all trivalent cations were assigned to $M(2)$, except in oxy-amphiboles; (iii) where Fe^{2+}/Fe^{3+} was not known, all Fe in $M(2)$ was assumed to be Fe^{3+}. This situation occurs for some hornblende'-type amphiboles where the Fe occupancy of $M(2)$ is small and chemical analyses of similar amphiboles show amounts of Fe^{3+} approximately equal to the $M(2)$ Fe occupancy of the amphiboles concerned. This is certainly not a general assumption for all amphiboles; (iv) except where Mössbauer and/or infrared evidence indicated otherwise, Mn was assumed to avoid $M(2)$ and was equally partitioned between $M(1)$ and $M(3)$.

Table 2 summarizes the data derived in this fashion from the amphiboles listed in Table 1*. As the ligancy and local environment of the three octahedral M sites differ considerably, the sites are best considered separately. Figure 2 shows the variation in mean bond length with

TABLE 2. MEAN BOND LENGTHS (Å) AND MEAN IONIC RADII (Å) OF THE CONSTITUENT IONS FOR THE THREE OCTAHEDRAL SITES IN THE CLINOAMPHIBOLES

	$\langle M(1){-}O\rangle$	$\langle r_{M(1)}\rangle$	$\langle M(2){-}O\rangle$	$\langle r_{M(2)}\rangle$	$\langle M(3){-}O\rangle$	$\langle r_{M(3)}\rangle$	$\langle r_{O(3)}\rangle$
Actinolite	2.106	0.760	2.096	0.728	2.098	0.758	1.339
Al-hastingsite	2.116	-	1.980	-	2.131	-	1.340
Cummingtonite	2.094	0.736	2.083	0.725	2.090	0.736	1.340
Ferrotschermakite	2.123	0.757	1.990	0.586	2.132	0.767	1.340
Glaucophane	2.087	0.730	1.943	0.541	2.094	0.737	1.340
Grunerite	2.121	0.771	2.121	0.766	2.113	0.773	1.329
K-richterite	2.063	0.717	2.092	0.727	2.054	0.713	-
Kaersutite	2.048	-	2.051	-	2.060	-	1.355
Kakanui hb.	2.077	0.741	2.047	0.662	2.079	0.741	-
Mn-cummingtonite	2.096	0.742	2.088	0.729	2.080	0.734	1.337
Na-Fe richterite	2.064	0.732	2.101	0.751	2.051	0.729	1.300
Na-richterite	2.053	0.720	2.085	0.720	2.057	0.720	1.300
Oxy-kaersutite	2.066	-	2.057	-	2.067	-	1.353
Pargasite	2.088	0.734	2.036	0.651	2.077	0.734	1.323
Ti-pargasite	2.081	0.739	2.048	0.664	2.084	0.739	-
Tremolite (F)	2.057	0.720	2.082	0.720	2.040	0.720	1.300
Tremolite (OH)	2.075	0.720	2.077	0.716	2.066	0.720	1.337
Tremolite	2.071	0.720	2.084	0.720	2.063	0.720	1.327
Zincian Tirodite	2.097	0.729	2.091	0.729	2.084	0.735	1.340

---

*A list of site-populations may be obtained from the Depository of Unpublished Data, CISTI, National Research Council of Canada, Ottawa, Canada, K1A 0S2.

the mean ionic radius of the constituent cations for the *M*(1), *M*(2) and *M*(3) sites, and the results of simple linear regression analyses are given in Table 3. The agreement for a linear model is excellent for *M*(2), but considerable scatter occurs for the *M*(1) and *M*(3) sites. This seems to be the result of the difference in ligancy at each site: *M*(2) is always coordinated by six oxygens and the constancy of the coordination results in good agreement with a simple linear model. Conversely, *M*(1) and *M*(3) are coordinated by four oxygens and two additional anions that may be OH^-, F^-, Cl^- or O^{2-}; some of the scatter exhibited by these sites in Figure 2 may be correlated with the mean ionic radius of the anion(s) occupying the O(3) position. This is illustrated by Figure 3 which shows the variation in mean bond length with O(3) anion radius for a mean cation radius of 0.720Å. In fifteen of the amphiboles of Table 1, the chemistry of the O(3) position is known with a fair degree of confidence; inclusion of the mean ionic radius of the O(3) anion as an independent variable in a stepwise linear regression analysis indicates that this factor contributes significantly to variations in the mean bond lengths of the *M*(1) and *M*(3) sites (Table 3). Some scatter still exists (Fig. 4) and may be due to an incorrect assignment of site-populations of such elements as Mn, Fe^{3+}, Ti^{3+} and Ti^{4+}. However, no conclusions can be drawn because other variations in O(3) chemistry have not been examined in most of the amphiboles of Table 1. It has been shown by Geijer (1959) and Leelanandam (1969a,b) that considerable amounts of Cl can occur in natural amphiboles. Cl^- is much larger than OH^- and even small amounts will

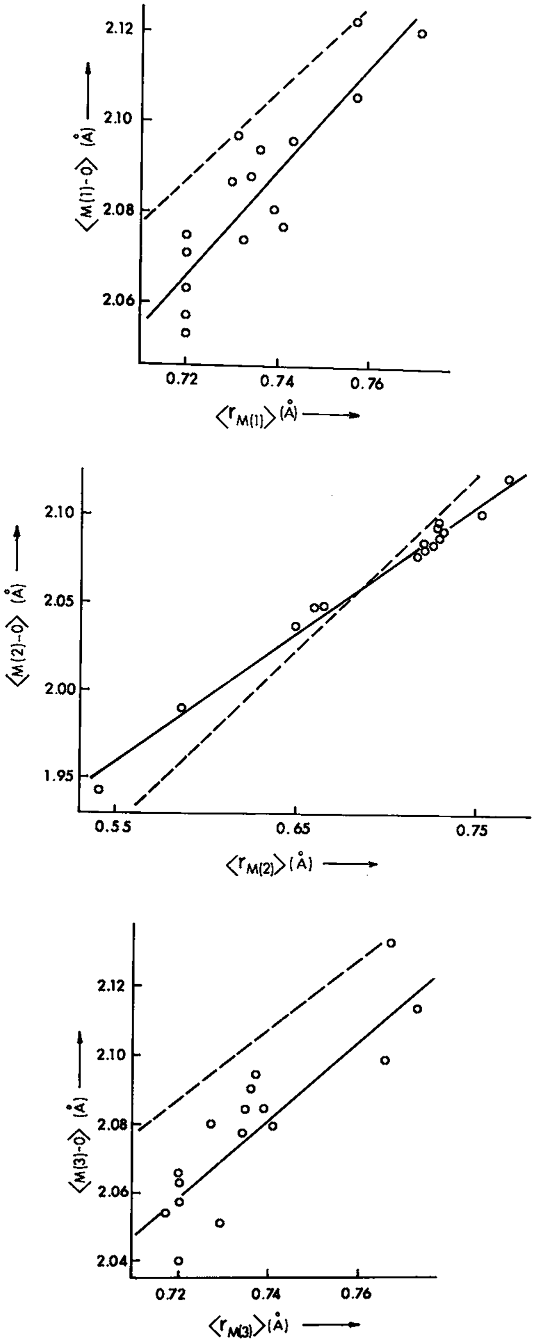

FIG. 2. Variation in mean bond length with mean ionic radius of the constituent cations at the octahedral sites in the clinoamphiboles. The full lines are the regression equations of Table 3; the dashed lines are the ideal relationships for the sum of the ionic radii.

TABLE 3. REGRESSION ANALYSIS RESULTS

	Dependent variable	Independent variable	c	m	R	σ	$\lvert t \rvert$[1]
1.	$\langle M(1)\text{-}O\rangle_{obs}$	$r_{M(1)}$	1.209	1.19(18)	0.870	0.011	6.59
2.	$\langle M(2)\text{-}O\rangle_{obs}$	$r_{M(2)}$	1.552	0.739(21)	0.995	0.005	35.02
3.	$\langle M(3)\text{-}O\rangle_{obs}$	$r_{M(3)}$	1.237	1.14(16)	0.884	0.011	7.09
4.	$\langle M(1)\text{-}O\rangle_{obs}$	$r_{M(1)}$ $r_{O(3)}$	0.556	0.94(9) 0.63(9)	0.979	0.005	9.75 6.49
5.	$\langle M(3)\text{-}O\rangle_{obs}$	$r_{M(3)}$ $r_{O(3)}$	0.604	0.90(14) 0.61(16)	0.950	0.008	6.33 3.69
6.	$\langle M(1)\text{-}O\rangle_{holo}$	$r_{M(1)}$ $r_{O(3)}$	0.516	0.94(9) 0.65(9)	0.979	0.005	9.61 6.67
7.	$\langle M(3)\text{-}O\rangle_{holo}$	$r_{M(3)}$ $r_{O(3)}$	0.681	0.75(9) 0.63(10)	0.966	0.006	7.25 5.22
8.	$\langle M(1)\text{-}O\rangle_{obs}$	$r_{M(1)}$ $r_{O(3)}$ $\lambda_{M(1)}$	-0.027	0.94(9) 0.64(9) 0.6(4)	0.982	0.005	10.12 6.82 1.31
9.	$\langle M(3)\text{-}O\rangle_{obs}$	$r_{M(3)}$ $r_{O(3)}$ $\lambda_{M(3)}$	-0.297	0.75(9) 0.56(10) 1.07(30)	0.979	0.006	6.92 4.87 3.49

[1] t values are calculated for the null hypothesis H_o:m=0.0

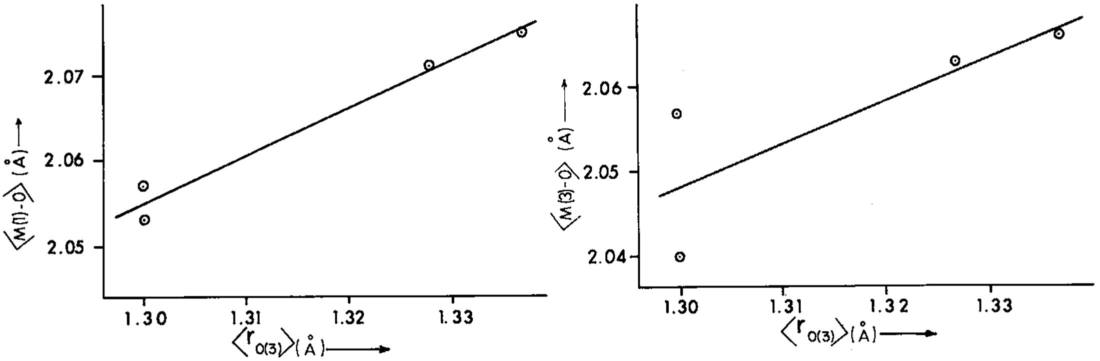

FIG. 3. Variations in mean bond length with mean ionic radius of the constituent O(3) anions(s) at the *M*(1) and *M*(3) sites for clinoamphiboles with $<r_{M(1)}> = <r_{M(3)}> = 0.720$Å.

significantly affect the mean bond length of the *M*(1) and *M*(3) sites; for example, an O(3) occupancy of $(OH_{.80}Cl_{.20})$ will lead to an increase in $<M(1)–O>$ and $<M(3)–O>$ of ~0.03Å over that occurring in the corresponding hydroxy-amphibole. In addition, whether significant amounts of O^{2-} can occur at O(3) in unoxidized amphiboles is not known; however, accurate methods of analysis have recently been developed (Wilkins & Sabine 1973) and this problem may soon be resolved. Because of these problems concerning the O(3) anion occupancies, extreme care must be taken in applying the relationships for *M*(1) and *M*(3) outlined in

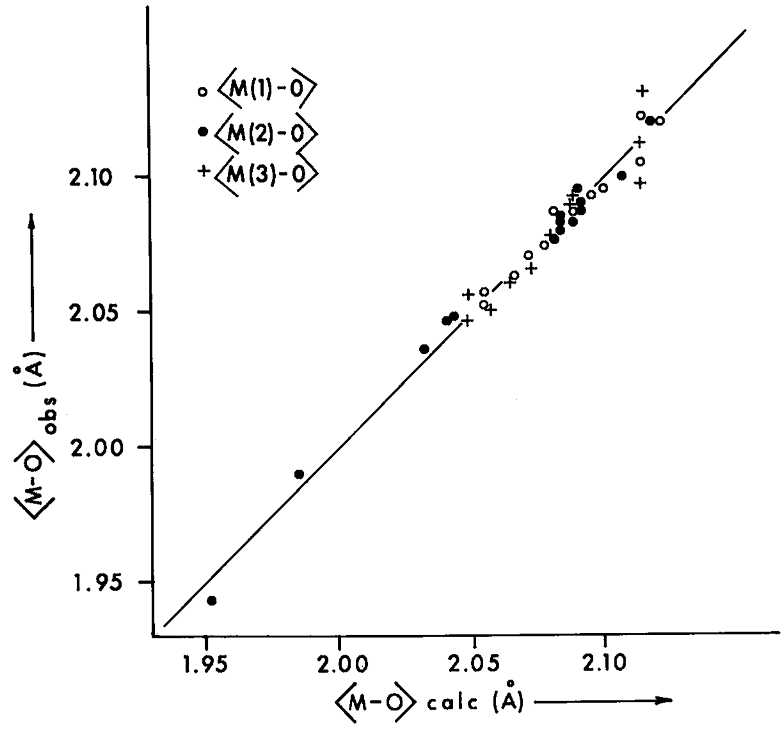

FIG. 4. Comparison of the observed mean bond lengths of the octahedral sites with the corresponding values calculated from the regression equations of Table 3 (nos. 2, 4 & 5).

Table 3 to the more complex natural amphiboles.

The results of the crystal structure refinement of the sub-silicic hastingsite (Hawthorne & Grundy 1977a) were not used in this analysis as there was no way of assessing the Fe^{3+} site-populations of the $M(1)$ and $M(3)$ sites. However, using the relationship developed above for $M(2)$, the forecast values for $\langle M(2)\text{–O}\rangle$ are 2.201 (Ti^{3+}) and 2.012 (Ti^{4+}), both of which are significantly greater than the observed value of 1.980(2)Å. There is a high degree of confidence in the X-ray results for the sub-silicic hastingsite as two separate refinements were performed on two separate crystals with virtually identical results. The analysis (Leake 1968, no. 932) is classed as superior and the $\langle T\text{–O}\rangle$ bond lengths confirm the unusual tetrahedral chemistry. The relationship between $\langle M(2)\text{–O}\rangle$ and $\langle r_{M(2)}\rangle$ is defined only by two data points in the region below $\langle r_{M(2)}\rangle = 0.65$Å; these are glaucophane and ferrotschermakite. In the refinement of glaucophane (Papike & Clark 1968), unconstrained site-population refinement resulted in a bulk chemistry that differed considerably from that indicated by the chemical analysis; in particular, the Al content of the $M(2)$ site was far greater than that indicated by the chemical analysis. Papike & Clark (1968) concluded that this difference was real, and that there was no reason why a single grain taken from a bulk sample should have the same composition as the bulk sample. Conversely, unconstrained site-population refinement can lead to considerable deviation of the total site-chemistry from that indicated by chemical analysis due to high parameter correlation in the least-squares procedure (Finger 1969; Burnham *et al.* 1971). Thus there is some question about the data point for glaucophane. With respect to ferrotschermakite, Figure 4 shows that the maximum deviations from the relationship for $M(1)$ and $M(3)$ occur for ferrotschermakite; it would appear that the cations occupying the $M(1)$ and $M(3)$ sites are too small. This casts some doubt upon the chemical analysis although in all other respects the refinement seems satisfactory. Because of the questions arising about the results for glaucophane and ferrotschermakite, the linear relationship for the $M(2)$ site below $\langle r_{M(2)}\rangle = 0.65$Å should not be considered as adequately established. Further experimental studies are planned in order to resolve this point.

Mean bond lengths in coordination polyhedra are sensitive to the degree of polyhedral distortion (Shannon & Calvo 1973a,b; Brown & Shannon 1973; Shannon 1976), and in principle, this could be a significant factor in apparent non-linearity between mean bond length and constituent-cation radius (Hawthorne & Ito 1977). The character of the octahedral distortions will be examined in the next section, but it is worthwhile considering the possible effect of distortion on mean bond length – ionic radius correlations in the amphiboles. Table 4 lists the distortional parameters Δ, λ and σ^2 (Appendix A) for the amphiboles of Table 1. There appears to be some correlation between the quadratic elongation, λ, and the deviation from linearity observed in the mean bond length – ionic radius correlations developed above. In an attempt to remove possible distortional effects, the above analysis was repeated using the bond length for a holosymmetric octahedron with the same volume as the experimentally observed octahedron. From the regression results of Table 3, there is a significant improvement in linearity for the $M(3)$ site but not for the $M(1)$ site. The improvement is particularly noticeable for those amphiboles showing extremely distorted bond angles (*e.g.*, ferrotschermakite) where large deviations (~0.015Å) in bond length – ionic radius relationships were observed (Fig. 4). A stepwise regression analysis was performed on the mean bond lengths, cation radius, O(3) anion radius and λ for the $M(1)$ and $M(3)$ sites; the results (Table 3) confirm the above result. Variations in λ seem to contribute significantly to variations in $\langle M(3)\text{–O}\rangle$ whereas they are not significant with respect to variation in $\langle M(1)\text{–O}\rangle$. Whether this represents some stereochemical difference between the $M(1)$ and $M(3)$ sites or whether the correlation for $M(3)$ is purely fortuitous must await further data and testing.

The stepwise regression analyses were repeated using the distortional parameter Δ (Brown & Shannon 1973); $|t|$-tests indicate that Δ does not contribute significantly to mean bond-length variations. This is not altogether surprising as a rough estimate of the increase in bond lengths due to distortion shows it generally to be negligible. From the bond-strength parameters and distortional equations given by Brown & Shannon (1973), the effect of octahedral distortion on the mean bond-lengths in amphibole octahedra is $\sim 6\Delta \times 10^{-4}$Å. Using the Δ values given in Table 4, the maximum deviations from the mean distortion for each site result in the following bond-length changes: $M(1)=0.013$Å, $M(2)=0.005$Å, $M(3)=0.001$Å; if the kaersutites are not included, the $M(1)$ value is reduced to 0.002Å. Thus it is not surprising that Δ is not significantly correlated with the changes in mean bond length.

TABLE 4. DISTORTIONAL PARAMETERS FOR THE OCTAHEDRAL SITES IN THE CLINOAMPHIBOLES

	M(1)				M(2)				M(3)			
	Δ	λ	σ^2	$\langle M(1)\text{-}O\rangle_{holo}$	Δ	λ	σ^2	$\langle M(2)\text{-}O\rangle_{holo}$	Δ	λ	σ^2	$\langle M(3)\text{-}O\rangle_{holo}$
Actinolite	0.30	1.0096	33.3	2.096Å	6.70	1.0068	22.7	2.089Å	0.03	1.0143	46.7	2.083Å
Al hastingsite	3.59	1.0203	65.3	2.095	6.87	1.0074	24.0	1.973	0.08	1.0347	111.1	2.095
Cummingtonite	1.57	1.0105	35.5	2.084	3.92	1.0096	31.2	2.074	0.34	1.0156	50.5	2.074
Ferrotschermakite	4.00	1.0181	57.3	2.104	5.00	1.0067	19.6	1.984	0.33	1.0328	106.0	2.098
Glaucophane	0.21	1.0204	69.5	2.066	15.77	1.0110	35.0	1.934	0.34	1.0262	85.0	2.067
Grunerite	2.25	1.0116	36.0	2.109	2.79	1.0130	43.2	2.108	0.11	1.0181	60.9	2.094
K-richterite	0.20	1.0131	43.1	2.050	14.57	1.0098	41.2	2.080	1.07	1.0149	47.6	2.039
Kaersutite	24.69	1.0221	56.4	2.028	9.44	1.0128	34.0	2.039	4.06	1.0276	79.4	2.032
Kakanui Hb.	4.96	1.0151	48.7	2.062	5.60	1.0088	27.3	2.039	0.13	1.0232	74.8	2.055
Mn cummingtonite	1.08	1.0107	33.8	2.085	5.90	1.0079	25.1	2.080	0.35	1.0127	42.3	2.067
Na-Fe richterite	0.90	1.0136	44.0	2.050	16.11	1.0128	37.4	2.089	1.37	1.0122	39.8	2.039
Na-richterite	0.62	1.0133	43.1	2.040	12.54	1.0108	33.1	2.075	0.97	1.0133	43.3	2.043
Oxy-kaersutite	14.35	1.0156	47.9	2.052	7.06	1.0098	31.2	2.048	0.05	1.0248	71.9	2.042
Pargasite	1.25	1.0160	50.5	2.072	5.98	1.0080	24.3	2.029	0.01	1.0237	75.7	2.053
Ti-pargasite	3.50	1.0145	47.0	2.066	6.13	1.0089	26.5	2.039	0.10	1.0236	75.5	2.060
Tremolite (F)	0.10	1.0146	46.9	2.042	5.75	1.0075	23.0	2.075	1.03	1.0150	47.9	2.025
Tremolite (OH)	0.15	1.0107	35.6	2.064	5.52	1.0069	22.9	2.070	0.09	1.0127	43.6	2.053
Tremolite	0.17	1.0115	37.2	2.059	6.05	1.0086	24.5	2.076	0.30	1.0141	44.8	2.049
Zincian tirodite	1.37	1.0104	32.9	2.087	6.34	1.0079	25.9	2.083	0.27	1.0134	43.1	2.071

Several interesting crystallochemical features emerge from the present study. The dashed lines in Figure 2 indicate the ideal relationships between mean bond length and ionic radius (*i.e.*, $\langle M\text{–}O\rangle = r_{\text{cation}} + r_{\text{anion}}$). For the data in Figure 2 and for the stepwise regression analyses of Table 3, the slopes of the experimentally derived relationships between mean bond length and cation radius for the *M*(1) and *M*(3) sites are not significantly different from unity, the ideal value for this model; however, the actual values are ~0.02Å less than the forecast values. Conversely, the slope of the experimentally derived relationship for the *M*(2) site (0.739) is considerably less than that expected, and the two curves intersect at ~0.64Å. This difference in slopes suggests that the *M*(2) site is 'held open' for small cations and compressed for large cations. This is quite reasonable in terms of the rest of the octahedral strip. The *c* repeat of the *M*(1)-*M*(3)-*M*(1)-*M*(3)-*M*(1) chain has to be equal to the *c* repeat of the *M*(1)-*M*(2)-*M*(1)-*M*(2)-*M*(1) chain; consequently, when a great disparity exists between the sizes of the *M*(2) and *M*(3) cations as is present when considerable Al occupies the *M*(2) site, the *M*(2) octahedron is held

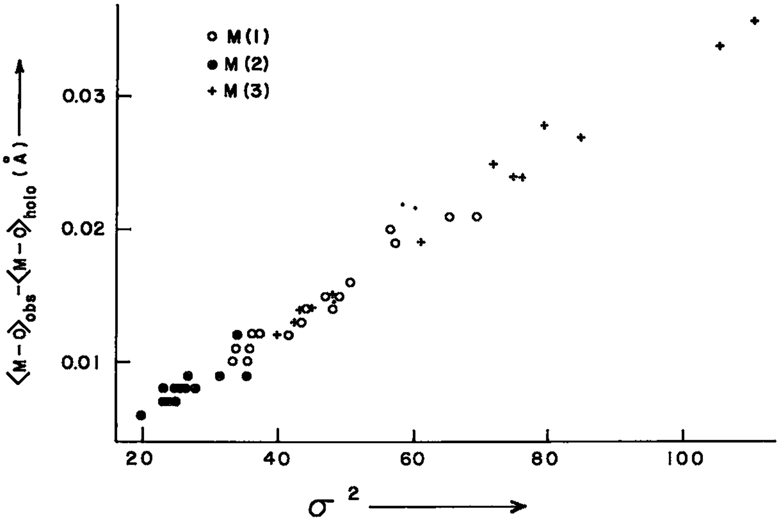

FIG. 5. The difference between the observed and 'holosymmetric' mean octahedral bond lengths as a function of the octahedral angle variance.

open by this requirement. As the size of the $M(2)$ cation increases, this effect decreases as the size difference between the $M(2)$ and $M(3)$ cations decreases. However, no explanation is proposed for the systematically short bond lengths observed in the amphiboles, although it should be noted that similar effects are apparent in the ortho- and clinopyroxenes.

It was noted previously that whereas λ is significantly correlated with changes in mean bond length, Δ is not. This is initially surprising as both parameters appear to represent bond-length distortion. Comparison of the difference between $\langle M\text{–O}\rangle_{obs}$ and $\langle M\text{–O}\rangle_{holo}$ (Table 4) with the octahedral angle variance, σ^2, (Fig. 5) reveals a very strong correlation; either bond-angle distortion affects mean bond lengths in crystals (an effect not recognized in crystals as yet), or deformation of polyhedra under the constraint of constant volume implies a relationship between angular distortion and strained centre-to vertex distances. One factor which suggests that the latter is not the case is that the geometry of the octahedra in amphiboles, as in many other solids, departs considerably from that allowed by homogeneous strain. The minimum point-symmetry of a homogeneously strained octahedron is $2/m\ 2/m\ 2/m$, and examination of the corresponding edge lengths of the octahedra in the amphiboles of Table 1 shows that extremely large departures from this symmetry are generally encountered. Simple geometrical arguments show that the observed differences in octahedral edge lengths that would be equivalent under $2/m\ 2/m\ 2/m$ symmetry can cause variations in the angles subtending these edges at the centre of the octahedron of the order of 10°, suggesting that any relationship between $\langle M\text{–O}\rangle_{holo}$ and σ^2 implicit in the assumption of homogeneous deformation should be obscured by departures from the minimum allowed symmetry.

The complete lack of correlation between Δ and σ^2 raises the question of how much λ is affected by individual bond-length deviations from the *observed* mean bond length. As $\lambda = 1/6 \sum_{i=1}^{6} (M\text{–O})_i / \langle M\text{–O}\rangle_{holo})^2$, it would seem that a comparison of λ and $(\langle M\text{–O}\rangle_{obs} / \langle M\text{–O}\rangle_{holo})^2$ would reveal to what extent λ is affected by individual bond-length variations. No significant difference was found between this quantity and λ. Thus λ does not represent deviations from the mean bond length but the difference between the observed mean bond length and $\langle M\text{–O}\rangle_{holo}$. The correlation between

TABLE 5. BOND STRENGTH* TABLES FOR SELECTED AMPHIBOLES

	M(1)	M(2)	M(3)	M(4)	A	T(1)	T(2)	Σ**	Σ		M(1)	M(2)	M(3)	M(4)	A	T(1)	T(2)	Σ**	Σ
	Tremolite: root mean square deviation = 4.13%										Glaucophane: root mean square deviation = 4.57%								
0(1)	.361	.307	.356			1.066		2.090	2.000	0(1)	.359	.370	.344			1.020		2.093	2.167
0(2)	.349	.345		.296			1.025	2.015	1.917	0(2)	.335	.471		.183			1.020	2.029	1.958
0(3)	.345$\overset{x2}{\rightarrow}$		.368					1.058	1.000	0(3)	.340$\overset{x2}{\rightarrow}$		.367					1.047	1.000
0(4)		.408		.359			1.116	1.883	1.583	0(4)		.604		.218			1.091	1.913	1.625
0(5)				.125		.981	.926	2.032	2.250	0(5)				.080		1.025	.967	2.072	2.125
0(6)				.209		.989	.880	2.078	2.250	0(6)				.169		1.011	.923	2.103	2.125
0(7)						1.025$\overset{x2}{\rightarrow}$		2.050	2.000	0(7)						1.040$\overset{x2}{\rightarrow}$		2.080	2.000
	Ferrohastingsite: root mean square deviation = 3.61%										Ferrotschermakite: root mean square deviation = 3.42%								
0(1)	.395	.391	.349			.928		2.063	2.024	0(1)	.395	.414	.335			.930		2.074	2.040
0(2)	.320	.408		.234			.989	1.951	1.995	0(2)	.305	.399		.281			.966	1.951	2.045
0(3)	.358$\overset{x2}{\rightarrow}$		.361					1.077	1.000	0(3)	.336$\overset{x2}{\rightarrow}$		.358					1.030	1.000
0(4)		.552		.277			1.067	1.896	1.662	0(4)		.517		.344			1.021	1.882	1.712
0(5)				.120	.070	.891	.944	2.025	2.189	0(5)				.164	.018	.869	.977	2.028	2.142
0(6)				.078	.055	.898	.891	2.022	2.189	0(6)				.216	.016	.901	.924	2.057	2.142
0(7)					.178	.928$\overset{x2}{\rightarrow}$		2.034	1.984	0(7)					.053	.962$\overset{x2}{\rightarrow}$		1.977	1.826
	Pargasite: root mean square deviation = 4.14%										Na-richterite: root mean square deviation = 6.01%								
0(1)	.383	.369	.365			.943		2.060	1.958	0(1)	.365	.271	.355			1.128		2.119	2.000
0(2)	.334	.365		.285			.987	1.971	2.000	0(2)	.392	.366		.238			1.000	1.996	1.854
0(3)	.346$\overset{x2}{\rightarrow}$		.361					1.053	1.000	0(3)	.276$\overset{x2}{\rightarrow}$		.300					.852	1.000
0(4)		.479		.329			1.052	1.860	1.667	0(4)		.412		.282			1.141	1.835	1.521
0(5)				.173	.058	.867	.957	2.055	2.208	0(5)				.089	.035	1.000	.914	2.038	2.271
0(6)				.199	.082	.894	.907	2.082	2.208	0(6)				.157	.027	.957	.859	2.000	2.271
0(7)					.154	.943$\overset{x2}{\rightarrow}$		2.040	1.950	0(7)					.047	.970$\overset{x2}{\rightarrow}$		1.987	2.200

[*] Calculated from the curves of Brown & Shannon (1973).

[**] The first summation column is the sum of the bond strengths shown in the table, the second column corresponding to the formal bond strength sums (Pauling 1960).

λ and σ^2 is extremely good; thus, as the bond angles become more distorted, the observed bond length increases relative to the holosymmetric bond length, irrespective of any individual bond-length variations. Perhaps λ represents changes in anion–anion interactions.

INDIVIDUAL BOND-LENGTH VARIATIONS

Deviations from Pauling's second rule (Pauling 1960) are accompanied by antipathetic variations in cation–anion distances (Zachariasen 1954, 1963; Evans 1960; Baur 1961, 1970, 1971). The recent development of bond strength – bond length relationships (Baur 1970, 1971; Donnay & Allmann 1970; Brown & Shannon 1973; Pyatenko 1973; Ferguson 1974) has indicated that bond-strength requirements are a major factor in controlling bond-length variations in inorganic structures. This will have an extremely strong effect on bond-length distortions in amphiboles as these minerals exhibit considerable deviations from Pauling's second rule for a formal bond-strength model. Bond-strength tables were calculated for the amphiboles listed in Table 1 using the curves of Brown & Shannon (1973) and Brown & Wu (1976). In Table 5, data for selected amphiboles are compared with the bond-strength sums calculated from the formal Pauling scheme. It is apparent that the bond-length distortions observed in the refined structures tend to minimize the devia-

TABLE 6. BOND LENGTHS FOR SELECTED AMPHIBOLES CALCULATED BY THE METHOD OF BAUR (1970, 1971)

	p_x	Δp_x	d^1_{calc}	d^2_{calc}	d_{obs}	$\Delta d^{1,2}$	$\Delta d^{1,3}$	p_x	Δp_x	d^1_{calc}	d^2_{calc}	d_{obs}	$\Delta d^{1,2}$	$\Delta d^{1,3}$
			Hydroxy-tremolite							Pargasite				
M(1)-0(1)	2.00	+0.027	2.090	2.078	2.064	-0.026	-0.014	1.98	-0.013	2.103	2.086	2.056	-0.047	-0.030
M(1)-0(2)	1.92	-0.053	2.080	2.069	2.078	-0.002	+0.009	2.00	+0.007	2.106	2.089	2.111	+0.005	+0.022
M(1)-0(3)	2.00	+0.027	2.090	2.078	2.083	+0.007	+0.005	2.00	+0.007	2.106	2.089	2.093	-0.009	+0.008
Mean	1.973		2.087	2.075	2.075			1.993		2.105	2.088	2.088		
M(2)-0(1)	2.00	+0.167	2.090	2.097	2.133	+0.043	+0.036	1.98	+ .100	2.013	2.053	2.069	+0.056	+0.016
M(2)-0(2)	1.92	+0.087	2.080	2.087	2.083	+0.003	-0.004	2.00	+ .120	2.017	2.057	2.074	+0.057	+0.017
M(2)-0(4)	1.58	-0.253	2.040	2.047	2.014	-0.026	-0.033	1.66	- .220	1.957	1.997	1.966	+0.009	-0.031
Mean	1.833		2.070	2.077	2.077			1.880		1.996	2.036	2.036		
M(3)-0(1)	2.00	0.000	2.090	2.066	2.070	-0.020	+0.004	1.98	-0.007	2.103	2.076	2.076	-0.027	0.000
M(3)-0.(3)	2.00	0.000	2.090	2.066	2.057	-0.033	-0.009	2.00	+0.013	2.106	2.079	2.080	-0.026	+0.001
Mean	2.00		2.090	2.066	2.066			1.987		2.104	2.077	2.077		
			Glaucophane (M(4)= [8])							Ferrohastingsite				
M(1)-0(1)	2.17	+0.127	2.126	2.106	2.078	-0.047	-0.028	2.02	+0.017	2.143	2.117	2.073	-0.070	-0.044
M(1)-0(2)	1.96	-0.083	2.095	2.075	2.082	-0.013	+0.007	1.99	-0.013	2.136	2.110	2.153	+0.017	+0.043
M(1)-0(3)	2.00	-0.043	2.101	2.081	2.100	-0.001	+0.019	2.00	-0.003	2.138	2.112	2.112	-0.026	0.000
Mean	2.043		2.107	2.087	2.087			2.003		2.139	2.113	2.113		
M(2)-0(1)	2.17	+0.250	1.959	2.003	2.038	+0.079	+0.035	2.02	+0.130	2.022	2.075	2.096	+0.074	+0.021
M(2)-0(2)	1.96	+0.040	1.909	1.953	1.943	+0.034	-0.010	1.99	+0.100	2.016	2.069	2.080	+0.064	+0.011
M(2)-0(4)	1.63	-0.290	1.830	1.874	1.849	+0.019	-0.025	1.66	-0.230	1.945	1.998	1.964	+0.019	-0.034
Mean	1.920	1.899	1.899	1.943	1.943			1.890		1.994	2.047	2.047		
M(3)-0(1)	2.17	+0.057	2.139	2.104	2.103	-0.036	-0.001	2.02	+0.007	2.153	2.128	2.130	-0.023	+0.002
M(3)-0(3)	2.00	-0.113	2.110	2.075	2.077	-0.033	+0.002	2.00	-0.013	2.147	2.122	2.117	-0.030	-0.005
Mean	2.113		2.129	2.094	2.094			2.013		2.151	2.126	2.126		
			Ferrotschermakite											
M(1)-0(1)	2.03	+0.017	2.140	2.127	2.067	-0.073	-0.060							
M(1)-0(2)	2.01	-0.003	2.135	2.122	2.170	+0.035	+0.048							
M(1)-0(3)	2.00	-0.013	2.133	2.120	2.131	-0.002	+0.011							
Mean	2.013		2.136	2.123	2.123									
M(2)-0(1)	2.03	+0.123	1.963	2.018	2.014	+0.051	-0.004							
M(2)-0(2)	2.01	+0.103	1.959	2.014	2.029	+0.070	+0.015							
M(2)-0(4)	1.68	-0.227	1.884	1.939	1.928	+0.044	-0.011							
Mean	1.907		1.935	1.990	1.990									
M(3)-0(1)	2.03	+0.010	2.152	2.134	2.141	-0.011	+0.007							
M(3)-0(3)	2.00	-0.020	2.145	2.127	2.115	-0.030	-0.012							
Mean	2.020		2.150	2.132	2.132									

Root Mean Square Deviations

	Δd^1	Δd^2
Tremolite	0.024	0.019
Pargasite	0.036	0.020
Glaucophane	0.040	0.020
Ferrotschermakite	0.047	0.029
Ferrohastingsite	0.047	0.027

---

[1] calculated from the realtionship $d=a+bp_x$ (Baur 1970) where d is the predicted bond length, p_x is the sum of the formal bond strengths received by the anion, and a and b are empirically derived constants.

[2] calculated from the relationship $d= \langle d_{obs} \rangle +b\Delta p_x$, where Δp_x is the bond strength sum deviation from the mean value received by the anions in a coordination polyhedra.

[3] $\Delta d=d_{obs}-d_{calc}$.

tions from ideality in the bond-strength sums around the anions. This is particularly significant with respect to cations coordinating the O(4) anion, all of which show extremely short bonds to O(4). To maintain mean bond lengths in accord with the size of the constituent cations, there is a concomitant lengthening of the other bond lengths, resulting in extremely distorted cation sites. This is evident from Table 4, which shows the distortional parameter Δ (Brown & Shannon 1973; Shannon & Calvo 1973a,b; Shannon 1976) for each of the octahedra. The relative degree of octahedral distortion is *M*(2)> *M*(1)>*M*(3), in agreement with the fact that *M*(2) is the only octahedral cation bonded to O(4). The one exception, oxykaersutite, has an extremely distorted *M*(1) octahedron because the O(3) position is occupied mainly by O^{2-}, necessitating extreme contraction of the *M*(1) – O(3) bonds (Hawthorne & Grundy 1973b) if the bond-strength requirements of the O(3) anion are to be satisfied. Extreme contraction of the *M*(3)–O(3) bonds cannot occur as the O(3) coordination of *M*(3) is in a *trans* rather than a *cis* arrangement, and linkage to the surrounding octahedra prevents this contraction; thus the *M*(3) octahedron in oxykaersutite remains fairly regular.

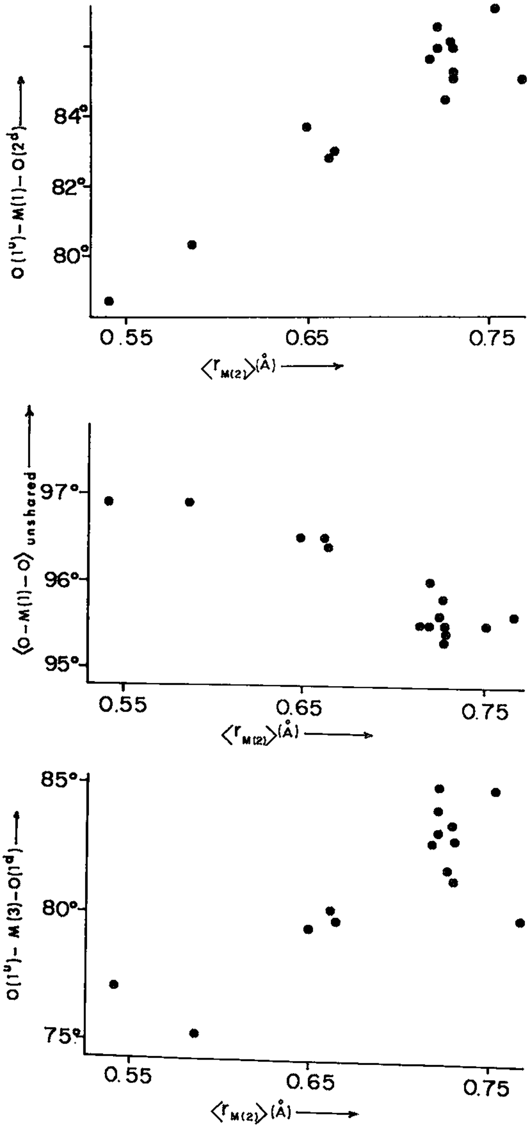

FIG. 6. Variation in various bond angles at the *M*(1) and *M*(3) sites with the mean ionic radius of the constituent *M*(2) cation(s).

It is also of interest to examine bond-length variations in the amphiboles using the formalism of Baur (1970, 1971) as, unlike the other bond-strength schemes mentioned above, it is used directly to predict bond lengths. In order to compare the results with those derived from the Brown & Shannon (1973) method, bond lengths were calculated for the same set of amphiboles with the exception of synthetic Mg-richterite, as the empirical constants necessary for this type of calculation are not available for the F anion. Baur's method may be used either to predict distances *a priori* (Baur 1970) or to predict the deviation of an individual bond length from the mean value of its coordination polyhedron (Baur 1971). Table 6 shows the bond-length calculations performed by both methods for five selected amphiboles. Certain features are immediately apparent upon inspection of the differences between the observed and calculated values. For the type 1 calculation, the bond lengths for the *M*(1) and *M*(3) octahedra are in general too large, in agreement with the feature noted earlier (Fig. 2a,c) that the mean bond lengths observed at these sites are significantly less than the sum of the relevant ionic radii. Conversely, the bond lengths for the *M*(2) octahedron are in general too small, and the deviation shows a partial correlation with the ionic radius of the *M*(2) cation. This agrees with the conclusion reached in the previous section that the <*M*(2)–O> bond lengths are significantly greater than the sum of the relevant ionic radii, and that the slope of the curve of <*M*(2)–O> versus $r_{M(2)}$ curve is unusually small.

Where the Δp_x values are large, Baur's method is quite successful in predicting the individual bond-length deviations from the mean. How-

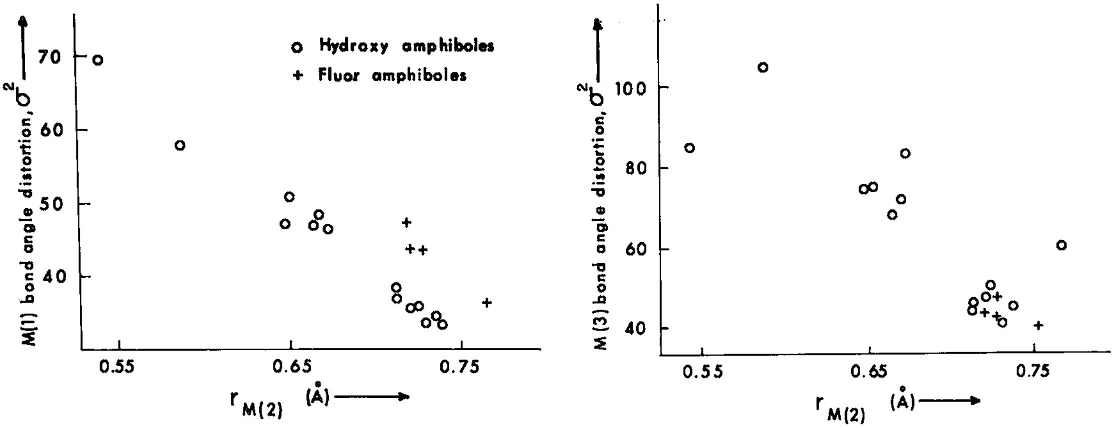

FIG. 7. Variation in $M(1)$ and $M(3)$ octahedral angle variance with the mean ionic radius of the constituent $M(2)$ cation(s).

ever, for small Δp_x values, the predicted deviation may be in the wrong sense. This is not surprising as the scheme is based on the premise that the sum of the 'distance-dependent' bond strengths should be equal to the magnitude of the anion valence and in general this rule does not provide sufficient constraints for the structure to be exactly defined. Thus additional features such as cation–cation repulsion and linkage constraints have a much greater proportional effect on bond-length variations involving anions with small Δp_x values.

BOND-ANGLE DISTORTIONS

It has been suggested (Pauling 1960) that cation–cation repulsive interactions are much stronger than anion-anion repulsive interactions, and that as a result, edges shared between polyhedra are shorter and subtend smaller angles at the cation than unshared edges. In the octahedral element of the clinoamphibole structure, the $M(1)$, $M(2)$ and $M(3)$ octahedra share six, five and six edges respectively with adjacent cation polyhedra, suggesting that cation-cation repulsion should play an important role in bond-angle distortion. Inspection of bond angles for the amphiboles listed in Table 1 shows that the bond angles generally conform to the above rule. However, certain exceptions indicate that additional factors affect bond-angle variation. Any differential variation in the size of edge-sharing octahedra must result in distortion of the 'bond angles' if the inter-octahedral linkages are to be maintained. As indicated in the previous section, there is considerable variation in the size of the octahedra in the clinoamphiboles with variation in cation occupancy. As the repeat distance along the $M(3)$-$M(1)$-$M(3)$ chain must be the same as that along the $M(2)$-$M(1)$-$M(2)$ chain, the cation occupancy of $M(2)$ may significantly affect the bond angles of the adjacent sites. Figure 6a shows the variation in $O(1^u)$-$M(1)$-$O(2^d)$ with the ionic radius of the constituent $M(2)$

TABLE 7. CALCULATED BOND ANGLES IN THE M(2) OCTAHEDRON OF SELECTED AMPHIBOLES

	Tremolite (OH)			Tremolite (F)			Na richterite		
	obs.		calc.	obs.		calc.	obs.		calc.
$O(1)$-$M(2)$-$O(1)$	80.0°		86.8°	80.0°		86.5°	79.7°		84.6°
$O(1^u)$-$M(2)$-$O(2^u)$	92.1	87.9	88.1	91.9	87.8	88.3	90.2	86.4	87.7
$O(1^u)$-$M(2)$-$O(2^d)$	83.7			83.7			82.6		
$O(1)$-$M(2)$-$O(4)$	92.8		89.9	92.6		89.7	91.0		88.9
$O(2^u)$-$M(2)$-$O(4^u)$	90.3	91.9	91.4	90.5	91.9	91.6	90.5	93.0	92.5
$O(2^u)$-$M(2)$-$O(4^d)$	93.4			93.3			95.6		
$O(4)$-$M(2)$-$O(4)$	95.0		93.4	95.5		93.2	99.1		94.0

cation; as expected, a significant positive correlation is exhibited, the bond angle contracting as the size of the *M*(2) octahedron decreases. Because the mean bond angle should remain constant, a condition that seems to hold for most inorganic crystal structures, other bond angles in the *M*(1) octahedron should expand. In order to avoid increasing cation-cation repulsion, this expansion should occur in the angles subtending unshared edges of the octahedron; Figure 6b shows that this is the case. A similar argument may be advanced concerning the bond angle variation in the *M*(3) octahedron; Figure 6c shows the variation in $O(1^u)–M(3)–O(1^d)$ with the ionic radius of the *M*(2) cation, and as with the *M*(1) octahedron, a reasonable positive correlation is exhibited. As the site symmetry of *M*(3) is 2/*m*, the $O(1^u)–M(3)–O(1^u)$ bond angle will show a negative correlation of the same magnitude. Thus the size of the *M*(2) cation does significantly affect the variation of some bond angles in the adjacent *M*(1) and *M*(3) octahedra. To what extent does this affect the overall bond-angle distortion at the *M*(1) and *M*(3) sites? This point is examined in Figure 7 where the variation in σ^2 is shown as a function of the mean ionic radius of the *M*(2) cation. Significant linear correlations are exhibited for both the *M*(1) and *M*(3) octahedra; the relationship for *M*(1) is particularly well-developed, with a slight offset in the data points of the fluor-amphiboles due to the perturbing effect of the smaller F anion.

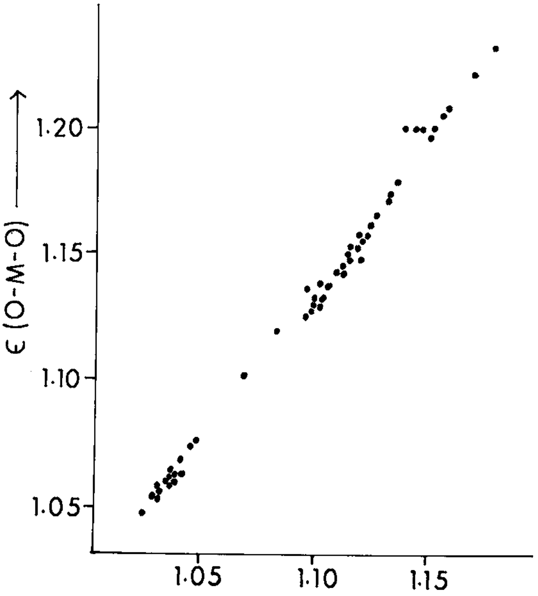

FIG. 8. Variation in the ratio of the mean bond angle involving unshared edges to the mean bond angle involving shared edges with the corresponding ratio for the edge lengths for the three octahedra in the clinoamphiboles.

It was shown in the previous section that considerable deviations from Pauling's second rule occur in the amphibole structures, and that the coordination polyhedra tend to distort so as to minimize these deviations. Whereas the *M*(1) and *M*(3) octahedra are coordinated by anions that do not show much deviation from Pauling's rule, the *M*(2) site is bonded to the O(4) anion that generally shows a large formal bond-strength deficiency. This leads to extremely distorted *M*(2) octahedra, with the *M*(2) cation being displaced away from the centre of the octahedron towards the O(4) anions. This displacement of the *M*(2) cation will lead to bond-angle changes that are an intrinsic result of the O(4) bond-strength requirements and not related to cation–cation repulsion or geometrical packing considerations. In order to assess the magnitude of these distortions, the bond angles were calculated for a holosymmetric octahedron with the observed bond lengths of hydroxy-tremolite, fluor-tremolite and fluor-richterite. In these three structures, the *M*(1), *M*(2) and *M*(3) cations are the same size, thus minimizing the effects of linkage between octahedra of disparate sizes. The results are given in Table 7 where they are compared with the observed values. It is apparent that the anion bond-strength requirements have a considerable effect on the bond-angle distortions at the *M*(2) site, even though comparison of the observed and calculated values indicate that additional distortions occur as a result of relaxation due to cation–cation repulsion. The effect of this may be seen by examining the amount of angular distortion in terms of the amount of relaxation due to cation–cation repulsion. To represent the amount of relaxation due to cation–cation repulsion, it is necessary to introduce another distortional index. The fact that the interaction is manifest on polyhedral edge lengths and angles suggests that the ratio of the mean values of the unshared and shared elements may be a representative index. Figure 8 shows the variation in this ratio for O-*M*-O angles with that for O-O distances at all three octahedra; the linearity exhibited is not geometrically implicit and both are formally independent of cation size. Either parameter could be used as the representative index; the angular ratio was chosen and is designated ϵ. Figure 9 shows the variation in σ^2 as a function of ϵ for the three octahedra in the clinoamphiboles. The correlations for *M*(1) and

$M(3)$ are fair whereas the variation for $M(2)$ is random. This may result from the additional angular distortions resulting from the anion bond-strength requirements, as outlined above and in Table 7.

There have been several attempts (Hawthorne 1973; Fleet 1974) to quantitatively characterize the amounut of relaxation due to cation-cation repulsion in the amphiboles. However, as shown above, other steric factors significantly affect bond angles and bond lengths, and their effects need to be quantitatively characterized before the relaxations resulting solely from cation–cation repulsion can be assessed. In addition, before any weight can be placed on this type of examination in the amphiboles, the same approach must be shown to be completely adequate for forecasting distortions in inorganic structures that do not show any deviation from Pauling's second rule.

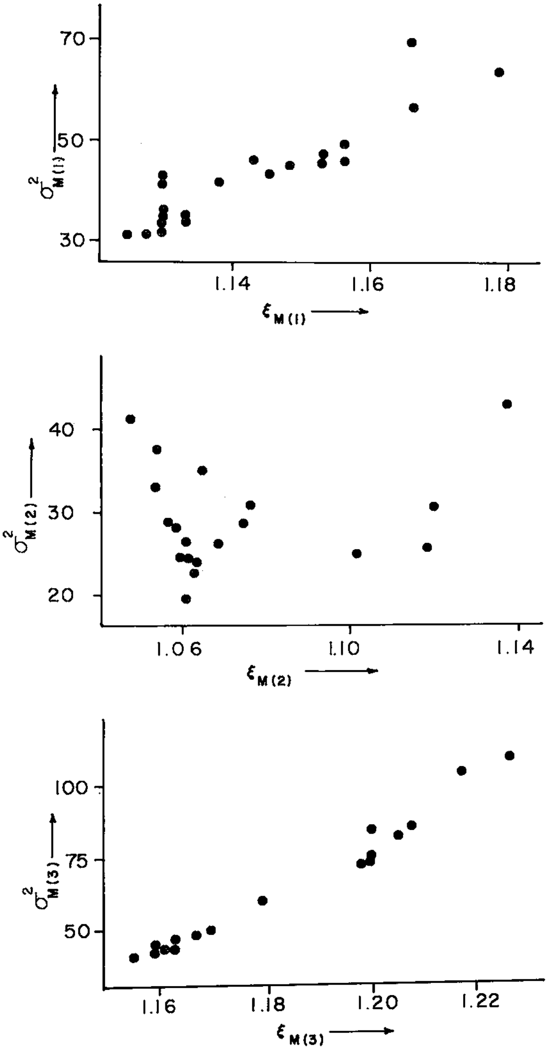

FIG. 9. Variation in ϵ (the ratio of the mean bond angle involving unshared edges to the mean bond angle involving shared edges) with σ^2 (octahedral angle variance) for the three octahedra in the clinoamphiboles.

ACKNOWLEDGEMENTS

Part of this work was excerpted from a doctoral dissertation submitted to the Department of Geology, McMaster University. I particularly thank Dr. H. D. Grundy for his help, advice and interest. Numerous people contributed towards this study in the form of discussions and arguments on amphiboles and crystal chemistry, and access to manuscripts prior to publication. In this regard, I thank Dr. I. D. Brown, Department of Physics, and Dr. C. Calvo, Department of Chemistry, both at McMaster University; Dr. R. B. Ferguson, Department of Earth Sciences, University of Manitoba; Mr. Ko Griep, itinerant scholar of no fixed abode, and Dr. R. D. Shannon, E. I. Dupont de Nemours, Wilmington, Delaware.

This work was supported by the University of Manitoba and the National Research Council of Canada (grants to R. B. Ferguson and H. D. Grundy).

REFERENCES

BAUR, W. H. (1961): Verzerrte Koordinationspolyeder in heteropolaren Kristallstrukturen und die elektrostatische Valenzregel von Pauling. *Naturwiss.* 48, 549-550.

——— (1970): Bond length variation and distorted coordination polyhedra in inorganic crystals. *Amer. Cryst. Assoc. Trans.* 6, 129-155.

——— (1971): The prediction of bond length variations in silicon–oxygen bonds. *Amer. Mineral.* 56, 1573-1599.

BORG, I. Y. (1967): On conventional calculations of amphibole formulae from chemical analyses with inaccurate H_2O (+) and F determinations. *Mineral. Mag.* 36, 583-590.

BROWN, G. E. (1970): *Crystal Chemistry of the Olivines*. Ph.D. thesis, Virginia Polytechnic Inst. & State Univ., Blacksburg, Va.

——— & GIBBS, G. V. (1969): Oxygen coordination and the Si-O bond. *Amer. Mineral.* 54, 1528-1539.

——— & ——— (1970): Stereochemistry and ordering in the tetrahedral portion of silicates. *Amer. Mineral.* **55**, 1587-1607.

Brown, I. D. & Shannon, R. D. (1973): Empirical bond strength – bond length curves for oxides. *Acta Cryst.* **A29**, 266-282.

——— & Wu, K. K. (1976): Empirical parameters for calculating cation–oxygen bond valences. *Acta Cryst.* **B32**, 1957-1959.

Burnham, C. W., Ohashi, Y., Hafner, S. S. & Virgo, D. (1971): Cation distribution and atomic thermal vibrations in an iron-rich orthopyroxene. *Amer. Mineral.* **56**, 850-876.

Burns, R. G. & Greaves, C. J. (1971): Correlations of infrared and Mössbauer site population measurements of actinolite. *Amer. Mineral.* **56**, 2010-2033.

Cameron, M. J. (1970): *The Crystal Chemistry of Tremolite and Richterite. A Study of Selected Anion and Cation Substitutions.* Ph.D. thesis, Virginia Polytechnic Inst. & State Univ., Blacksburg, Va.

——— & Gibbs, G. V. (1971): Refinement of the crystal structures of two synthetic fluor-richterites. *Carnegie Inst. Wash. Year Book* **70**, 150-153.

——— & ——— (1973): The crystal structure and bonding of fluor-tremolite: a comparison with hydroxyl tremolite. *Amer. Mineral.* **58**, 879-888.

Donnay, G. & Allmann, R. (1970): How to recognize O^{2-}, OH^- and H_2O in crystal structure determined by X-rays. *Amer. Mineral.* **55**, 1003-1015.

Evans, H. T. (1960): Crystal structure refinement and vanadium bonding in the metavanadates KVO_3, NH_4VO_3 and $KVO_3{\cdot}H_2O$. *Z. Krist.* **114**, 257-277.

Ferguson, R. B. (1974): A cation–anion distance-dependent method for evaluating valence–bond distributions in ionic structures and results for some olivines and pyroxenes. *Acta Cryst.* **B30**, 2527-2539.

Finger, L. W. (1967): *The Crystal Structures and Crystal Chemistry of Ferromagnesian Amphiboles.* Ph.D. thesis, University of Minnesota, Minneapolis, Minn.

——— (1969): The crystal structure and cation distribution of a grunerite. *Mineral. Soc. Amer. Spec. Pap.* **2**, 95-100.

——— (1970): Refinement of the crystal structure of an anthophyllite. *Carnegie Inst. Wash. Year Book* **68**, 283-288.

——— & Zoltai, T. (1967): Cation distribution in grunerite. *Amer. Geophys. Union Trans.* **48**, 233-234 (Abstr.).

——— & Ohashi, Y. (1974): Preliminary results of the refinement of the crystal structure of holmquistite. *Carnegie Inst. Wash. Year Book* **73**, 535-539.

Fischer, K. F. (1966): A further refinement of the crystal structure of cummingtonite, $(Mg,Fe)_7(Si_4O_{11})_2(OH)_2$. *Amer. Mineral.* **51**, 814-818.

Fleet, M. E. (1974): Distortions in the coordination polyhedra of *M* site atoms in olivines, clinopyroxenes and amphiboles. *Amer. Mineral.* **59**, 1083-1093.

Geijer, P. (1959): The distribution of halogens in skarn amphiboles in central Sweden. *Arkiv Min. Geol.* **2**, 481-503.

Ghose, S. (1961): The crystal structure of a cummingtonite. *Acta Cryst.* **14**, 622-627.

——— (1965): A scheme of cation distributions in the amphiboles. *Mineral. Mag.* **35**, 46-54.

Gibbs, G. V. (1969): The crystal structure of protoamphibole. *Mineral. Soc. Amer. Spec. Pap.* **2**, 101-110.

Greaves, C., Burns, R. G. & Bancroft, G. M. (1971): Resolution of actinolite Mössbauer spectra into three ferrous doublets. *Nature* **229**, 60-61.

Hawthorne, F. C. (1973): *The Crystal Chemistry of the Clino-amphiboles.* Ph.D. thesis, McMaster University, Hamilton, Ontario.

——— (1976): The crystal chemistry of the amphiboles. V. The structure and chemistry of arfvedsonite. *Can. Mineral.* **14**, 346-356.

——— & Grundy, H. D. (1973a): The crystal chemistry of the amphiboles. I. Refinement of the crystal structure of ferrotschermakite. *Mineral. Mag.* **39**, 36-48.

——— & ——— (1973b): The crystal chemistry of the amphiboles. II. Refinement of the crystal structure of oxykaersutite. *Mineral. Mag.* **39**, 390-400.

——— & ——— (1973c): The crystal structure and site chemistry of a zinc manganese cummingtonite by least-squares refinement of single-crystal X-ray and Mössbauer data. *Amer. Mineral.* **58**, 1103 (Abstr.).

——— & ——— (1974): Refinement of the crystal structure of $NaScSi_2O_6$. *Acta Cryst.* **B29**, 2615-2616.

——— & ——— (1976): The crystal chemistry of the amphiboles: IV. X-ray and neutron refinements of the crystal structure of tremolite. *Can. Mineral.* **14**, 334-345.

——— & ——— (1977a): The crystal chemistry of the amphiboles: III. Refinement of the crystal structure of a sub-silicic hastingsite. *Mineral. Mag.* **41**, 43-50.

——— & ——— (1977b): The crystal structure and site-chemistry of a zincian tirodite by least-squares refinement of X-ray and Mössbauer data. *Can. Mineral.* **15**, 309-320.

——— & ——— (1977c): Refinement of the crystal structure of $LiScSi_2O_6$. *Can. Mineral.* **15**, 50-58.

——— & Ito, J. (1977): Synthesis and crystal-structure refinement of transition-metal orthopyroxenes. I: Orthoenstatite and (Mg,Mn,Co) orthopyroxene. *Can. Mineral.* **15**, 321-338.

IRUSTETA, M. C. & WHITTAKER, E. J. W. (1975): A three-dimensional refinement of the structure of holmquistite. *Acta Cryst.* **B31**, 145-150.

KITAMURA, M. & TOKONAMI, M. (1971): The crystal structure of kaersutite. *Sci. Rep. Tohoku Univ. Ser. 3*, **11**, 125-141.

———, ——— & MORIMOTO, N. (1975): Distribution of titanium atoms in oxy-kaersutite. *Contr. Mineral. Petrology* **51**, 167-172.

LEAKE, B. E. (1968): A catalogue of analyzed calciferous and subcalciferous amphiboles together with their nomenclature and associated minerals. *Geol. Soc. Amer. Spec. Pap.* **98**.

LEELANANDAM, C. (1969a): Electron microprobe analyses of chlorine in hornblendes and biotites from the charnockitic rocks of Kondapalli, India. *Mineral. Mag.* **37**, 362-365.

——— (1969b): Fluorine and chlorine in the charnockitic hornblendes from Kondapalli, India. *Neues Jahrb. Mineral. Monatsh.* **8**, 379-383.

LYONS, P. C. (1976): The chemistry of riebeckites of Massachusetts and Rhode Island. *Mineral. Mag.* **40**, 473-479.

MITCHELL, J. T. (1970): *Crystal Structure Refinement of Actinolite.* M.S. thesis, Virginia Polytechnic Inst. & State Univ., Blacksburg, Va.

———, BLOSS, F. D. & GIBBS, G. V. (1970): The variation of tetrahedral bond lengths and angles in clinoamphibole. *Geol. Soc. Amer. Program Abstr.* **2**, 626.

———, ——— & ——— (1971): Examination of the actinolite structure and four other *C2/m* amphiboles in terms of double bonding. *Z. Krist.* **133**, 273-300.

NOVAK, G. A. & GIBBS, G. V. (1971): The crystal chemistry of the silicate garnets. *Amer. Mineral.* **56**, 791-825.

PAPIKE, J. J. & CLARK, J. R. (1967): Crystal-chemical role of potassium and aluminum in a hornblende of proposed mantle origin. *Geol. Soc. Amer. Spec. Pap.* **115**, 171 (Abstr.).

——— & ——— (1968): The crystal structure and cation distribution of glaucophane. *Amer. Mineral.* **53**, 1156-1173.

——— & ROSS, M. (1970): Gedrites: Crystal structures and intra-crystalline cation distributions. *Amer. Mineral.* **55**, 1945-1972.

———, ——— & CLARK, J. R. (1969): Crystal chemical characterization of clinoamphiboles based on five new structure refinements. *Mineral. Soc. Amer. Spec. Pap.* **2**, 117-136.

PAULING, L. (1960): *The Nature of the Chemical Bond.* 3rd Ed., Cornell Univ. Press, Ithaca, N.Y.

PYATENKO, YU. A. (1973): Unified approach to analysis of the local balance of valences in inorganic structures. *Soviet Physics Cryst.* **17**, 677-682.

ROBINSON, K. (1971): *The Crystal Structures of Zircon, Clinohumite and the Hornblendes. A Determination of Polyhedral Distortion and Order-Disorder.* Ph.D. thesis, Virginia Polytechnic Inst. & State Univ., Blacksburg, Va.

———, GIBBS, G. V. & RIBBE, P. H. (1969): A refinement of the crystal structure of pargasite. *Amer. Mineral.* **55**, 307 (Abstr.).

———, ——— & ——— (1971): Quadratic elongation. A quantitative measure of distortion in coordination polyhedra. *Science* **172**, 567-570.

———, ———, ——— & HALL, M. R. (1973): Cation distribution in three hornblendes. *Amer. J. Sci.* **273A**, 522-535.

SEIFERT, F. & VIRGO, D. (1974): Temperature dependence of intracrystalline Fe^{2+}-Mg distribution in a natural anthophyllite. *Carnegie Inst. Wash. Year Book* **73**, 405-411.

SHANNON, R. D. (1976): Revised effective ionic radii and systematic studies of interatomic distances in halides and chalcogenides. *Acta Cryst.* **A32**, 751-757.

——— & CALVO, C. (1973a): Refinement of the crystal structure of synthetic chervetite, $Pb_2V_2O_7$. *Can. J. Chem.* **51**, 70-76.

——— & ——— (1973b): Refinement of the crystal structure of low temperature Li_3VO_4 and analysis of mean bond lengths in phosphates, arsenates and vanadates. *J. Solid State Chem.* **6**, 538-549.

——— & PREWITT, C. T. (1969): Effective ionic radii in oxides and fluorides. *Acta Cryst.* **B25**, 925-946.

——— & ——— (1970): Revised values of effective ionic radii. *Acta Cryst.* **B26**, 1046-1048.

THOMPSON, J. B. (1970): Geometrical possibilities for amphibole structures. Model biopyriboles. *Amer. Mineral.* **55**, 292-293.

WHITTAKER, E. J. W. (1949): The structure of Bolivian crocidolite. *Acta. Cryst.* **2**, 312-317.

——— (1969): The structure of the orthorhombic amphibole holmquistite. *Acta Cryst.* **B25**, 394-397.

——— (1971): Madelung energies and site preferences in amphiboles. I. *Amer. Mineral.* **56**, 980-996.

WILKINS, R. W. T. & SABINE, W. (1973): Water content of some nominally anhydrous silicates. *Amer. Mineral.* **58**, 508-516.

ZACHARIASEN, W. H. (1954): Crystal chemical studies of the 5F-series of elements, XXIII. On the crystal chemistry of uranyl compounds and of related compounds of transuranic elements. *Acta Cryst.* **7**, 795-807.

——— (1963): The crystal structure of cubic metaboric acid. *Acta Cryst.* **16**, 380-384.

Received March 1977; revised manuscript accepted September 1977.

APPENDIX: GLOSSARY OF SYMBOLS

$<M\text{–}O>$ observed mean bond length. Where this is used in conjunction with the next two symbols, it will be designated by the subscript *obs* for clarity.

$<M\text{–}O>_{\mathrm{calc}}$ calculated mean bond length.

$<M\text{–}O>_{\mathrm{holo}}$ The centre-to-vertex distance of a holosymmetric octahedron (point symmetry $4/m\bar{3}2/m$) of the same volume as the corresponding distorted octahedron.

$<\mathrm{r}_M>$ mean ionic radius of the cations occupying the *M* site.

Δ octahedral distortion parameter (Brown & Shannon 1973), defined by $\Delta = \sum_{i=1}^{6} [((M\text{–}\mathrm{O})_i - <M\text{–}\mathrm{O}>)/<M\text{–}\mathrm{O}>]^2/6 \times 10^4$.

λ quadratic elongation (Robinson *et al.* 1971), defined by $\lambda = \sum_{i=1}^{6}](\mathrm{M–O})/<\mathrm{M–O}>_{\mathrm{holo}}]^2/6$.

σ^2 octahedral angle variance (Robinson *et al.* 1971), defined by $\sigma^2 = \sum_{i=1}^{12} (\theta_i - 90)^2/11$.

ϵ angular distortion index to represent relaxation due to cation-cation repulsion, defined by $\epsilon = <\mathrm{O}\text{–}M\text{–}\mathrm{O}>_u/<\mathrm{O}\text{–}M\text{–}\mathrm{O}>_s$, where the subscripts *u* and *s* respectively represent unshared and shared elements.

p_x sum of the bond strengths received by an anion according to the electrostatic valence rule (Baur 1971).

$\Delta\ p_x$ difference between the p_x of one individual anion in a coordination polyhedron around a cation and the $<P_x>$ of all anions in this coordination (Baur 1970, 1971).

d_{calc} calculated bond lengths using the equations of Baur (1970).

Δd difference between the observed and calculated (d_{calc}) bond lengths.